

# HEAT TRANSFER EFFECTS OF THERMAL RADIATION ON A NANOFLUID FLOW PAST AN OSCILLATING VERTICAL PLATE WITH VARIABLE TEMPERATURE IN THE PRESENCE OF ROTATION

A. Antony Gnana Aravind and J. Ravikumar

MSC 2020 Classifications: 74F05; 76U05; 80A21; 82D80.

Keywords and phrases: Oscillating vertical plate, heat transfer, nanofluids, thermal radiation.

J. Ravikumar\* Corresponding author.

**Abstract** The effects of heat radiation on a nanofluid's flow passing through an oscillating vertical plate at different nanofluids and temperatures are the main subject of the investigation.  $CuO$ ,  $ZnO$ , and  $TiO_2$  are among the water-based nanofluids for which analytical solutions are produced. The method of Laplace transform is employed to resolve the dimensionless governing equations. The research examines how velocity profiles impact several physical characteristics, such as time, thermal Grashof number, rotational parameter, radiational parameter, and Prandtl number. The results are shown using graphs.  $ZnO$ -water,  $CuO$ -water, and  $TiO_2$ -water have similar velocity patterns that may be interpreted by their almost equal densities, which raises questions about the importance of this result. The comparison of these three nanoparticles reveals that  $TiO_2$ -water has a high velocity whereas  $CuO$ -water and  $ZnO$ -water have low velocities and also compared the various phase angles, radiations, rotations, and temperatures of these three nanoparticles.

## 1 Introduction

Traditional heat transfer fluids, such as oil, water, and blends containing ethylene glycol, exhibit insufficient heat transfer capabilities due to their low thermal conductivity. Utilizing these fluids for cooling purposes leads to increased manufacturing and operational expenses. Engine heat dissipation from automobiles is improved and overall efficiency is raised by nanofluids' increased thermal conductivity in coolant fluids. Nanofluids improve performance and longevity by reducing overheating and facilitating greater heat dissipation in electronics such as CPUs and GPUs. In order to increase heat exchange efficiency and lower energy consumption, nanofluids are utilized in HVAC systems. Nanofluids are explored in cooling systems for batteries and supercapacitors to maintain optimal operating temperatures, enhancing performance and safety. Magnetic nanofluids, such as  $Fe_3O_4$ , are used in biomedical applications for targeted medication delivery and hyperthermia therapy, assisting in the localized heating of malignant cells. Nanofluids are used to cool high-precision medical equipment such as MRI machines, ensuring steady functioning.

To enhance the thermal conductivity of these fluids, The experimentation of nanoparticles being incorporated into liquids has been investigated by researchers [2]. Nanofluids are produced via the application of energy to nanoparticles with a size of around 100 nm, which are contained inside a base fluid, such as water or a chemical solvent [8]. When it comes to conductivity, heating, and convectional heat transfer, nanofluids outperform conventional fluids [4]. Nanofluids find diverse applications across industries and engineering disciplines, including chemical synthesis, solar panel and power plant cooling, transformer oil cooling, microelectronics fabrication, the development of nano-drug delivery, microfluidics research, transportation breakthroughs, biomedical developments, and solid-state lighting technologies; the cooling of automobiles and air conditioners; the creation of sophisticated nuclear systems [5].

[1] explored the impact of varying the viscosity and thermal conductivity of a  $CuO$ -water

nanofluid on natural convection. Through mathematical modeling and simulations, the researchers investigated many elements of nanofluid flow and heat transmission under a variety of situations. In [3], the study focused on the behavior of parabolic flow passing a rapidly moving, isothermal vertical plate, considering the effects of heat and mass diffusion as well as plate rotation. [10] utilized an oscillating porous flat plate inside a rotating system in order to investigate the impact that heat radiation and Hall effects have on magnetohydrodynamic free convective nanofluid flow. [11] investigated the application of water-based nanofluids containing  $TiO_2$ ,  $ZnO$ , and  $SiO_2$  in thermal analyses of fuel cells. [9] evaluated the efficiency of single basin, single slope solar stills utilizing different water-based nanofluids. Additionally, [12] carried out a comprehensive study on the thermal conductivity of nanoparticles dispersed in a base fluid.

[7] employed an exact solution to study taking into consideration changes in temperature, mass diffusion, and heat radiation when submerging a vertical plate in a spinning fluid. [13] demonstrated the thermodynamic instability of nanofluids in the context of natural convection. Recent research by [6] focused on the influence of  $ZnO$  nanoparticles on the thermo-physical properties and heat transfer characteristics of nanofluid flows. [14] research was conducted to study the effect that heat radiation plays in an uneven flow of nanofluid across a vertical plate. Additionally, [15] explored the combined effects of radiation absorption and microwave heating on a vertically oriented plate that was exponentially accelerated, with variable temperature and concentration.

[16] conducted a study on the unsteady free convection flow of a nanofluid over a moving vertical plate, considering constant heat and mass flux. [17] investigated double-diffusive hydromagnetic natural convection in a hybrid nanofluid ( $TiO_2$ -Cu/Water) flowing past an infinite vertical plate, incorporating the effects of viscous dissipation and thermal radiation. Additionally, [18] carried out numerical simulations to analyze thermal energy preservation in hybrid nanofluids, taking into account chemical behavior, viscous dissipation, and the influence of inclination.

As far as the authors know, no other research has been done on how an unstable spinning nanofluid flows past a vertical plate that moves back and forth and has a temperature that changes while thermal radiation is present. This investigation aims to investigate the impact of thermal radiation on the free convective rotational flow of a nanofluid along an oscillating vertical plate with a temperature gradient passing through it. The Laplace transform technique is used to get solutions to the dimensionless version of the system's nonlinear partial differential equations. The research focuses on three water-based nanofluids containing zinc oxide ( $ZnO$ ), copper oxide ( $CuO$ ), and titanium dioxide ( $TiO_2$ ) nanoparticles. Closed-form analytical solutions are derived for the governing equations, and a comprehensive analysis is conducted to evaluate the impact of various parameters, such as the thermal radiation parameter, Grashof number, Prandtl number, and experimental time, on the temperature and velocity profiles. Graphical representations are provided to illustrate these effects.

## 2 Mathematical Analysis

This study studies the viscous flow of a rotating nanofluid that is incompressible across an oscillating vertical plate that has a changeable temperature. Additionally, the effects of thermal radiation are taken into consideration into the investigation. The flow is non-uniform and occurs past an infinite vertical plate at a constant ambient temperature  $T_\infty$ . Specifically, the coordinate system is established in such a way that the axes  $x'$  and  $y'$  are perpendicular to the surface of the plate, while the axis  $z'$  is parallel to the plane of the plate. The plate is observed from a fixed vertical position along the  $x'$  axis. Both the fluid and the plate rotate uniformly around the  $z'$ -axis with an angular velocity  $\Omega'$ .

At the initial time  $t' = 0$ , both the plate and the fluid are at the same temperature,  $T_\infty$ . For  $t' > 0$ , the plate is heated to a temperature  $T_w$  by applying a force that drives it within its plane against gravitational forces. It is also assumed that the plate experiences radiative heat transfer, denoted as  $q_r$ , in the direction perpendicular to its surface. The nanofluid consists of water mixed with three types of nanoparticles: silver ( $Ag$ ), aluminum oxide ( $Al_2O_3$ ), and titanium dioxide ( $TiO_2$ ). Additionally, it is assumed that the temperature of the nanoparticles suspended in the base fluid matches the temperature of the nanofluid itself. The thermophysical properties of the

nanofluids are detailed in Table 1.

Physical Propertie	Water and nanoparticle thermophysical properties			
	Water/Base Fluid	TiO <sub>2</sub>	CuO	ZnO
$\rho$ (kg/m <sup>3</sup> )	997.1	4250	6500	5606
$c_p$ (J/(kgK))	4179	686.2	540	667
$K$ (W/mK)	0.613	8.9538	18	13
$\beta \times 10^5$ (K <sup>-1</sup> )	21	0.9	0.85	4.7
$\phi$	0.0	0.1	0.15	0.2

The following equations govern the unsteady flow according to the traditional Boussinesq’s approximation:

$$\rho_{nf} \left( \frac{\partial u'}{\partial t'} - 2\Omega' v' \right) = g(\rho\beta)_{nf}(T - T_\infty) + \mu_{nf} \frac{\partial^2 u'}{\partial z'^2} \tag{2.1}$$

$$\rho_{nf} \left( \frac{\partial v'}{\partial t'} + 2\Omega' u' \right) = \mu_{nf} \frac{\partial^2 v'}{\partial z'^2} \tag{2.2}$$

$$(\rho C_p)_{nf} \frac{\partial T}{\partial t'} = k_{nf} \frac{\partial^2 T}{\partial z'^2} - \frac{\partial q_r}{\partial z'} \tag{2.3}$$

Here,  $u$  represents the velocity component along the  $x$ -axis,  $v$  represents the velocity component along the  $y$ -axis, and  $T$  denotes the temperature of the nanofluid. The dynamic viscosity of the nanofluid is represented by  $\mu_{nf}$ , the thermal expansion coefficient by  $\beta_{nf}$ , the density by  $\rho_{nf}$ , and the thermal conductivity by  $k_{nf}$ . The acceleration due to gravity is denoted by  $g$ , the radiative heat flux by  $q_r$ , and the heat capacitance of the nanofluid by  $(\rho c_p)_{nf}$ . These properties are defined as follows:

$$\mu_{nf} = \frac{\mu_f}{(1 - \phi)^{2.5}}, \quad \rho_{nf} = (1 - \phi)\rho_f + \phi\rho_s$$

$$(\rho c_p)_{nf} = (1 - \phi)(\rho c_p)_f + \phi(\rho c_p)_s, \quad (\rho\beta)_{nf} = (1 - \phi)(\rho\beta)_f + \phi(\rho\beta)_s \tag{2.4}$$

Here,  $\phi$  represents the solid volume fraction of the nanoparticles,  $\rho_f$  denotes the density of the base fluid,  $\rho_s$  is the density of the nanoparticles,  $\mu_f$  is the viscosity of the base fluid,  $(\rho C_p)_f$  is the heat capacitance of the base fluid, and  $(\rho C_p)_s$  is the heat capacitance of the nanoparticles. It is important to note that expressions (2.1) and (2.2) are specifically valid for spherical nanoparticles and do not apply to nanoparticles of other shapes. The effective thermal conductivity of the nanofluid is determined using the Hamilton and Crosser model.

$$k_{nf} = k_f \left( \frac{k_s + 2k_f - 2\phi(k_f - k_s)}{k_s + 2k_f + \phi(k_f - k_s)} \right) \tag{2.5}$$

Here,  $k_f$  represents the thermal conductivity of the base fluid, and  $k_s$  denotes the thermal conductivity of the nanoparticles. In equations (2.1)–(2.5), the subscripts  $_{nf}$ ,  $_f$ , and  $_s$  correspond to the thermophysical properties of the nanofluid, base fluid, and nanoparticles, respectively.

The initial and boundary conditions for the proposed problem are defined as follows:

$$\begin{aligned} &u' = 0, \quad v' = 0, \quad T = T_\infty \quad \text{for all } z', \quad t' \leq 0 \\ t' > 0 : &u' = u_0 \cos(\omega' t'), \quad v' = 0, \quad T = T_\infty + (T_w - T_\infty) A t' \quad \text{at } z' = 0 \\ &u' \rightarrow 0, \quad v' \rightarrow 0, \quad T \rightarrow T_\infty \quad \text{as } z' \rightarrow \infty \end{aligned} \tag{2.6}$$

Where  $A = \frac{u_0^2}{\nu}$ .

When the following dimensionless quantities are introduced, they become:

$$\begin{aligned}
 (u, v) &= \left( \frac{u'}{u_0}, \frac{v'}{u_0} \right), \quad t = \frac{t'(u_0)^2}{\nu_f}, \quad z = \frac{z'u_0}{\nu_f}, \quad Pr = \frac{\mu c_p}{k_f}, \\
 \theta &= \frac{T - T_\infty}{T_w - T_\infty}, \quad \Omega = \frac{\Omega'\nu}{(u_0)^2}, \quad \omega = \frac{\omega'\nu}{(u_0)^2}, \quad Gr = \frac{g\nu_f\beta(T_w - T_\infty)}{(u_0)^3}, \\
 R &= \frac{16a^*\sigma(T_\infty)^3}{k_f} \left( \frac{\nu_f^2}{(u_0)^2} \right)
 \end{aligned} \tag{2.7}$$

The local radiant in the case of an optically thin gray gas is represented by

$$\frac{\partial q_r}{\partial z'} = -4a^*\sigma(T_\infty^4 - T^4) \tag{2.8}$$

$T^4$  is approximated as a linear function of temperature due to the small temperature variations within the flow. This simplification is achieved by expanding  $T^4$  in a Taylor series around  $T_\infty$  and neglecting higher-order terms, resulting in:

$$T^4 \cong 4T_\infty^3 T - 3T_\infty^4 \tag{2.9}$$

By using equations (2.8) and (2.9), equation (2.3) reduces to

$$(\rho C_p)_{nf} \frac{\partial T}{\partial t} = k_{nf} \frac{\partial^2 T}{\partial z^2} + 16a^*\sigma T_\infty^3 (T_\infty - T) \tag{2.10}$$

The expression  $q = u + iv$  is a complex velocity,  $i = \sqrt{-1}$  in equations (2.1),(2.2),(2.3) and (2.6). By using equations (2.4),(2.5) and (2.7), equations (2.1) and (2.10) leads to:

$$A_1 \left( \frac{\partial q}{\partial t} + 2i\Omega \right) = A_3 \frac{\partial^2 q}{\partial z^2} + A_2 Gr \theta \tag{2.11}$$

$$A_4 \frac{\partial \theta}{\partial t} = A_5 \frac{1}{Pr} \frac{\partial^2 \theta}{\partial z^2} - \frac{R}{Pr} \theta \tag{2.12}$$

Where:

$$\begin{aligned}
 A_1 &= (1 - \phi) + \phi \left( \frac{\rho_s}{\rho_f} \right), \quad A_2 = (1 - \phi) + \phi \left( \frac{(\rho\beta)_s}{(\rho\beta)_f} \right), \quad A_3 = \frac{1}{(1 - \phi)^{2.5}} \\
 A_4 &= (1 - \phi) + \phi \left( \frac{(\rho c_p)_s}{(\rho c_p)_f} \right), \quad A_5 = \frac{k_f (k_s + 2k_f - 2\phi(k_f - k_s))}{k_s + 2k_f + 2\phi(k_f - k_s)}
 \end{aligned}$$

Here,  $Gr$  represents the thermal Grashof number,  $Pr$  denotes the Prandtl number, and  $R$  signifies the radiation parameter. When  $R \rightarrow 0$ , it indicates the absence of radiation effects, whereas a large value of  $R$  implies a dominant radiation influence.

The dimensionless initial and boundary conditions are as follows:

$$\begin{aligned}
 t = 0, & \quad q = 0, & \theta &= 0 & \text{for all } z, t \leq 0 \\
 t > 0: & \quad q = \cos(\omega t), & \theta &= t & \text{at } z = 0 \\
 & \quad q \rightarrow 0, & \theta &\rightarrow 0 & \text{as } z \rightarrow \infty
 \end{aligned} \tag{2.13}$$

The dimensionless governing equations (2.11) and (2.12) are solved using the standard Laplace transform method, applying the initial and boundary conditions specified in (2.13). The following solutions are obtained:

$$\begin{aligned}
 \theta &= \frac{t}{2} \left[ \exp(-2\eta\sqrt{a}\sqrt{bt}) \operatorname{erfc}(\eta\sqrt{a} - \sqrt{bt}) + \exp(2\eta\sqrt{a}\sqrt{bt}) \operatorname{erfc}(\eta\sqrt{a} + \sqrt{bt}) \right] \\
 &\quad - \frac{\eta\sqrt{at}}{\sqrt{b}} \left[ \exp(-2\eta\sqrt{a}\sqrt{bt}) \operatorname{erfc}(\eta\sqrt{a} - \sqrt{bt}) - \exp(2\eta\sqrt{a}\sqrt{bt}) \operatorname{erfc}(\eta\sqrt{a} + \sqrt{bt}) \right]
 \end{aligned} \tag{2.14}$$

$$\begin{aligned}
 q = & \frac{1}{4} \exp(i\omega t) \left[ \exp \left( 2\eta\sqrt{e}\sqrt{i\omega t + gt} \right) \operatorname{erfc} \left( \eta\sqrt{e} + \sqrt{i\omega t + gt} \right) \right. \\
 & + \left. \exp \left( -2\eta\sqrt{e}\sqrt{i\omega t + gt} \right) \operatorname{erfc} \left( \eta\sqrt{e} - \sqrt{i\omega t + gt} \right) \right] \\
 & + \frac{1}{4} \exp(-i\omega t) \left[ \exp \left( 2\eta\sqrt{e}\sqrt{-i\omega t + gt} \right) \operatorname{erfc} \left( \eta\sqrt{e} + \sqrt{-i\omega t + gt} \right) \right. \\
 & + \left. \exp \left( -2\eta\sqrt{e}\sqrt{-i\omega t + gt} \right) \operatorname{erfc} \left( \eta\sqrt{e} - \sqrt{-i\omega t + gt} \right) \right] \\
 & - \frac{c}{2d^2} \left[ \exp \left( 2\eta\sqrt{e}\sqrt{gt} \right) \operatorname{erfc} \left( \eta\sqrt{e} + \sqrt{gt} \right) + \exp \left( -2\eta\sqrt{e}\sqrt{gt} \right) \operatorname{erfc} \left( \eta\sqrt{e} - \sqrt{gt} \right) \right] \\
 & - \frac{c}{d} \left[ \frac{t}{2} \left[ \exp \left( 2\eta\sqrt{e}\sqrt{gt} \right) \operatorname{erfc} \left( \eta\sqrt{e} + \sqrt{gt} \right) + \exp \left( -2\eta\sqrt{e}\sqrt{gt} \right) \operatorname{erfc} \left( \eta\sqrt{e} - \sqrt{gt} \right) \right] \right. \\
 & \left. - \frac{\eta\sqrt{et}}{\sqrt{g}} \left[ \exp \left( -2\eta\sqrt{e}\sqrt{gt} \right) \operatorname{erfc} \left( \eta\sqrt{e} - \sqrt{gt} \right) - \exp \left( 2\eta\sqrt{e}\sqrt{gt} \right) \operatorname{erfc} \left( \eta\sqrt{e} + \sqrt{gt} \right) \right] \right] \\
 & + \frac{c}{d^2} \frac{\exp(dt)}{2} \left[ \exp \left( 2\eta\sqrt{e}\sqrt{(d+g)t} \right) \operatorname{erfc} \left( \eta\sqrt{e} + \sqrt{(d+g)t} \right) \right. \\
 & + \left. \exp \left( -2\eta\sqrt{e}\sqrt{(d+g)t} \right) \operatorname{erfc} \left( \eta\sqrt{e} - \sqrt{(d+g)t} \right) \right] \\
 & + \frac{c}{2d^2} \left[ \exp \left( 2\eta\sqrt{a}\sqrt{bt} \right) \operatorname{erfc} \left( \eta\sqrt{a} + \sqrt{bt} \right) + \exp \left( -2\eta\sqrt{a}\sqrt{bt} \right) \operatorname{erfc} \left( \eta\sqrt{a} - \sqrt{bt} \right) \right] \\
 & + \frac{c}{d} \left[ \frac{t}{2} \left[ \exp \left( 2\eta\sqrt{a}\sqrt{bt} \right) \operatorname{erfc} \left( \eta\sqrt{a} + \sqrt{bt} \right) + \exp \left( -2\eta\sqrt{a}\sqrt{bt} \right) \operatorname{erfc} \left( \eta\sqrt{a} - \sqrt{bt} \right) \right] \right. \\
 & \left. - \frac{\eta\sqrt{at}}{\sqrt{b}} \left[ \exp \left( -2\eta\sqrt{a}\sqrt{bt} \right) \operatorname{erfc} \left( \eta\sqrt{a} - \sqrt{bt} \right) - \exp \left( 2\eta\sqrt{a}\sqrt{bt} \right) \operatorname{erfc} \left( \eta\sqrt{a} + \sqrt{bt} \right) \right] \right] \\
 & - \frac{c}{d^2} \frac{\exp(dt)}{2} \left[ \exp \left( 2\eta\sqrt{a}\sqrt{(b+d)t} \right) \operatorname{erfc} \left( \eta\sqrt{a} + \sqrt{(b+d)t} \right) \right. \\
 & + \left. \exp \left( -2\eta\sqrt{a}\sqrt{(b+d)t} \right) \operatorname{erfc} \left( \eta\sqrt{a} - \sqrt{(b+d)t} \right) \right]
 \end{aligned}$$

Where,

$$a = \frac{A_4 \operatorname{Pr}}{A_5}, \quad b = \frac{R}{A_4 \operatorname{Pr}}, \quad c = \frac{Gr A_2}{a A_3 - A_1}, \quad d = \frac{g A_1 - ab A_3}{a A_3 - A_1}, \quad e = \frac{A_1}{A_3}, \quad g = 2i\Omega, \quad \eta = \frac{z}{2\sqrt{t}},$$

*erfc* is the error complimentary function.

The error function and complementary error function involve complex arguments. The term *q*, which represents a complex velocity, is decomposed into its real and imaginary components using the following expression:

$$\begin{aligned}
 \operatorname{erf}(x + iy) = & \operatorname{erf}(x) + \frac{\exp(-x^2)}{2x\pi} [1 - \cos(2xy) + i \sin(2xy)] \\
 & + \frac{2 \exp(-x^2)}{\pi} \sum_{n=1}^{\infty} \frac{\exp\left(-\frac{n^2}{4}\right)}{n^2 + 4x^2} [f_m(x, y) + i g_m(x, y)] + \epsilon(x, y)
 \end{aligned}$$

Where,

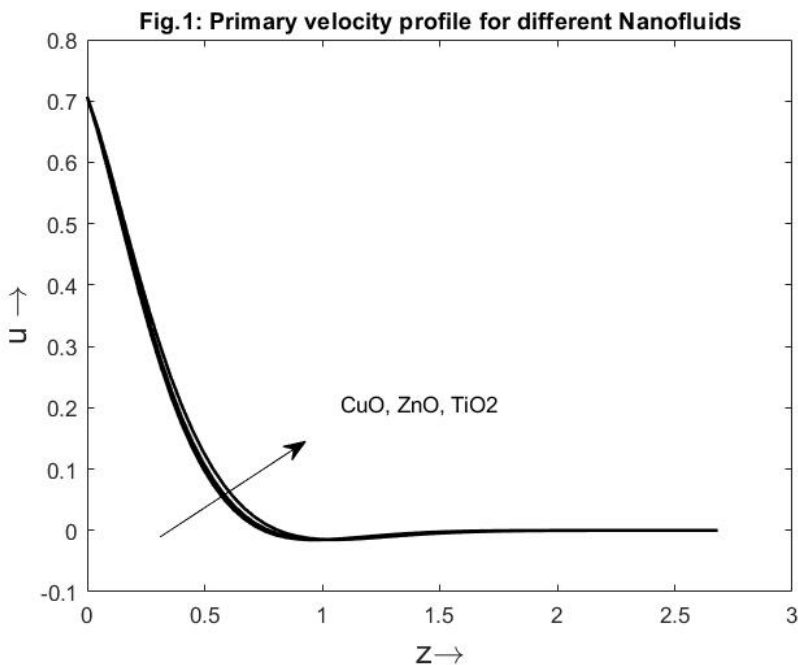
$$\begin{aligned}
 f_m &= 2x - 2x \cosh(my) \cos(2xy) + m \sinh(my) \sin(2xy) \\
 g_m &= 2x \cosh(my) \sin(2xy) + m \sinh(my) \cos(2xy) \\
 |\epsilon(x, y)| &\approx 10^{-16} |\operatorname{erf}(x + iy)|
 \end{aligned}$$

### 3 Results and Discussion

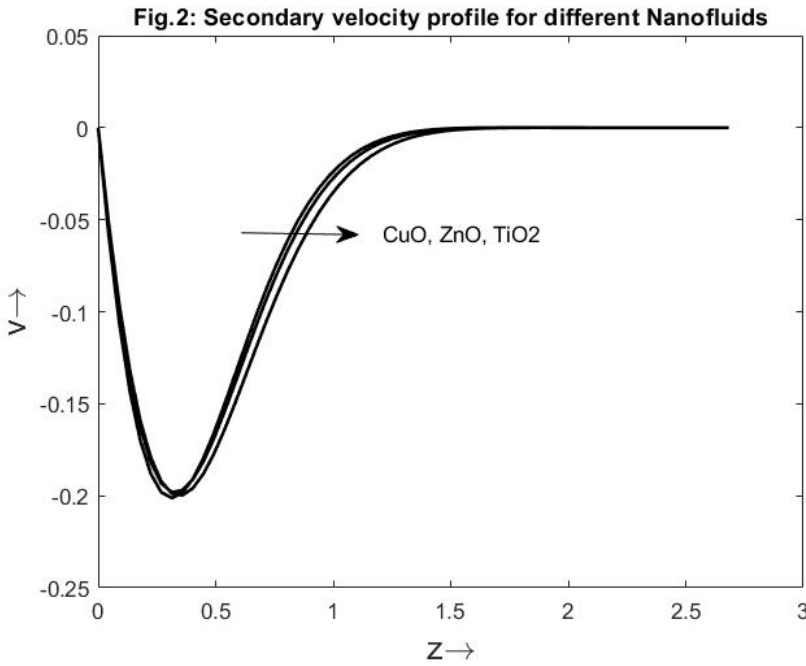
Detailed computations are carried out for various values of the thermophysical parameters, and the results are graphically presented to provide a comprehensive understanding of the fundamental physical aspects of the problem. The study focuses on three types of nanofluids containing zinc oxide ( $ZnO$ ), copper oxide ( $CuO$ ), and titanium dioxide ( $TiO_2$ ) nanoparticles. The volume fraction of nanoparticles is varied within the range  $0 \leq \phi \leq 0.2$ . The case  $\phi = 0$  represents the base fluid, where nanoparticle effects are absent.

Figure 1 illustrates the primary velocity profiles for different nanoparticles ( $ZnO$ ,  $CuO$ , and  $TiO_2$ ) at a constant solid volume fraction  $\phi = 0.1$ , with parameters  $Gr = 5$ ,  $Pr = 6.2$ ,  $R = 5$ ,  $\omega t = \pi/4$ ,  $\Omega = 0.5$ , and  $t = 0.2$ . The similar velocity distributions of  $ZnO$ -water and  $CuO$ -water can be attributed to their comparable densities. However, the higher density of  $TiO_2$  results in greater dynamic viscosity for  $TiO_2$ -water, leading to a thinner boundary layer compared to the other nanoparticles.

Figure 2 depicts the secondary velocity profiles for the same nanoparticles ( $ZnO$ ,  $CuO$ , and  $TiO_2$ ) under identical conditions:  $\phi = 0.1$ ,  $Gr = 5$ ,  $Pr = 6.2$ ,  $R = 5$ ,  $\omega t = \pi/4$ ,  $\Omega = 0.5$ , and  $t = 0.2$ . The results indicate that  $CuO$ -water and  $ZnO$ -water exhibit lower velocities, while  $TiO_2$ -water demonstrates higher velocity due to its distinct thermophysical properties.



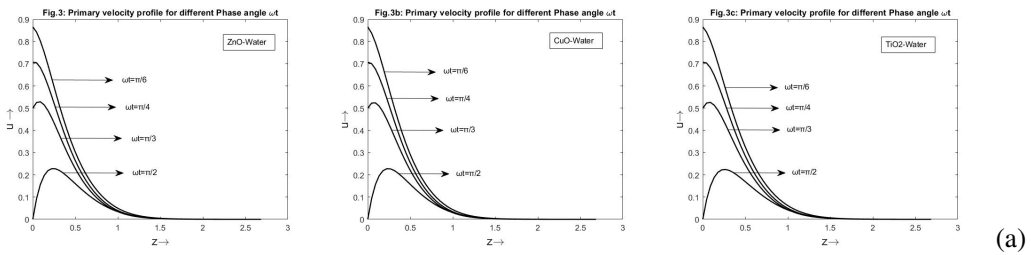
**Figure 1.** Primary Velocity Profile for various Nanofluids



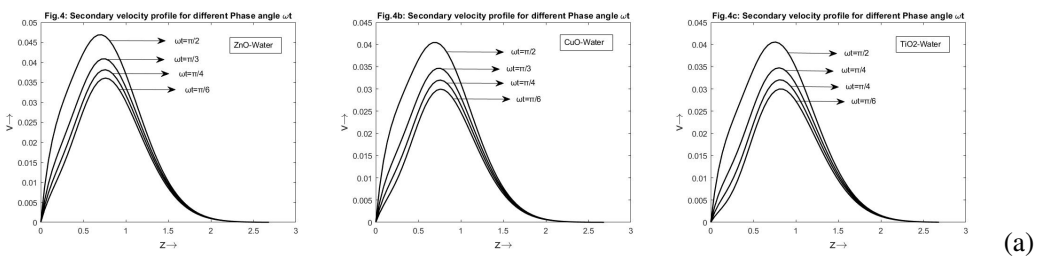
**Figure 2.** Secondary Velocity Profile for various Nanofluids

The primary and secondary velocity profiles of nanofluids are analyzed for varying values of the phase angle, radiation parameter, and rotation parameter, as depicted in Figures 3 to 8. These simulations are conducted under constant conditions:  $Pr = 6.2$ ,  $Gr = 5$ ,  $\phi = 0.1$ , and  $t = 0.2$ .

Figure 3 demonstrates that the primary velocity ( $u$ ) increases as the phase angle  $\omega t$  decreases. Conversely, Figure 4 shows that the secondary velocity ( $v$ ) increases with an increase in the phase angle  $\omega t$ .



ZnO (b) CuO (c) TiO<sub>2</sub> Primary Velocity Profile for different  $\omega t$



ZnO (b) CuO (c) TiO<sub>2</sub> Secondary Velocity Profile for different  $\omega t$

Figure 5 demonstrates a positive correlation between the primary velocity ( $u$ ) and the radiation parameter  $R$ , showing that an increase in  $R$  results in an increase in the primary velocity  $u$ . On the other hand, Figure 6 illustrates that the secondary velocity ( $v$ ) increases as the radiation parameter  $R$  decreases.

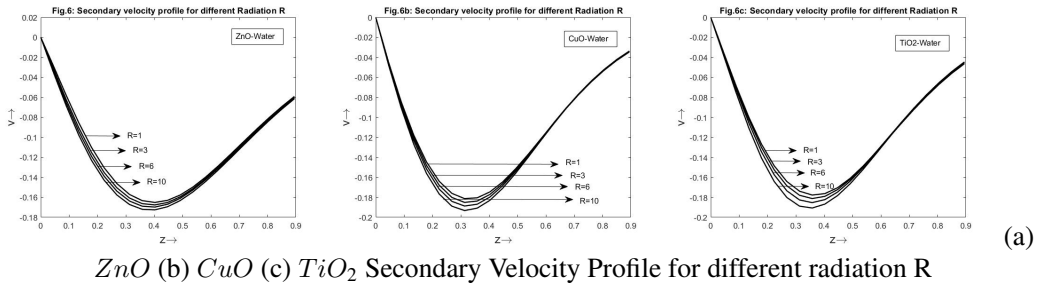
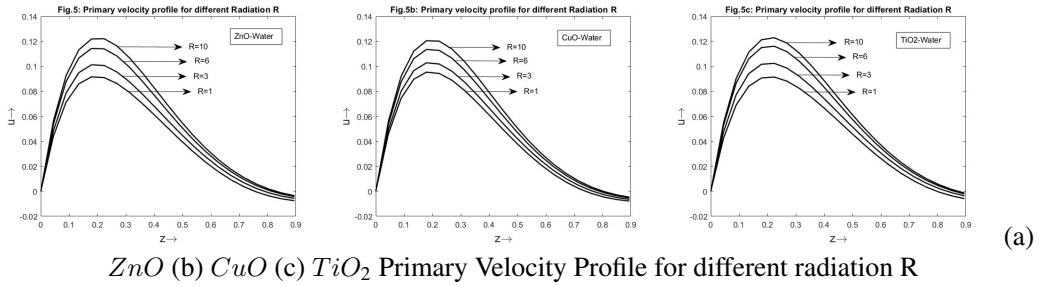


Figure 7 shows that the primary velocity ( $u$ ) increases as the rotation parameter ( $\Omega$ ) decreases. Similarly, Figure 8 indicates that the secondary velocity ( $v$ ) also increases with a decrease in the rotation parameter ( $\Omega$ ).

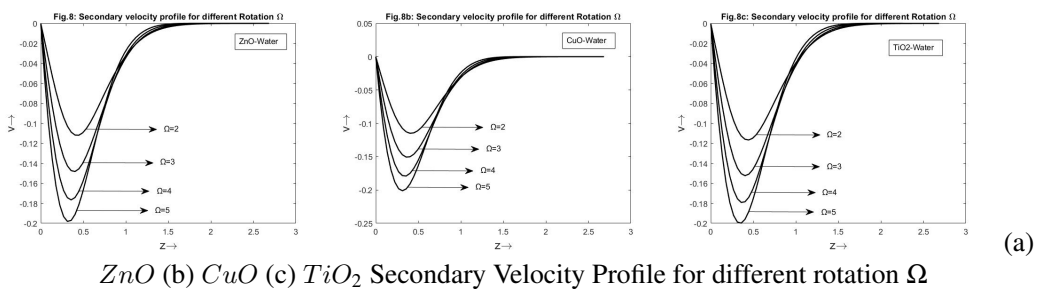
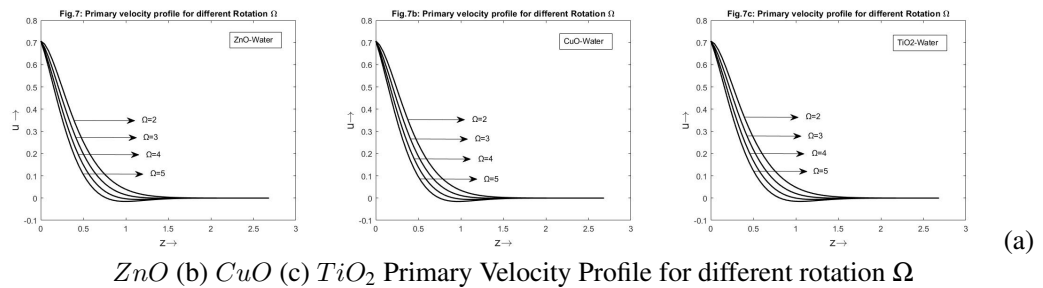
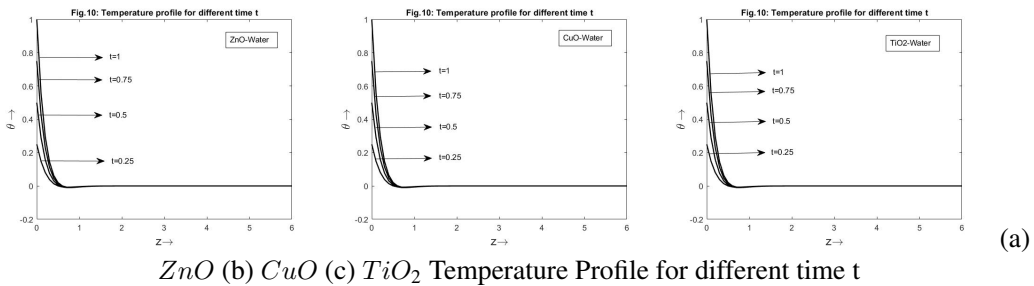
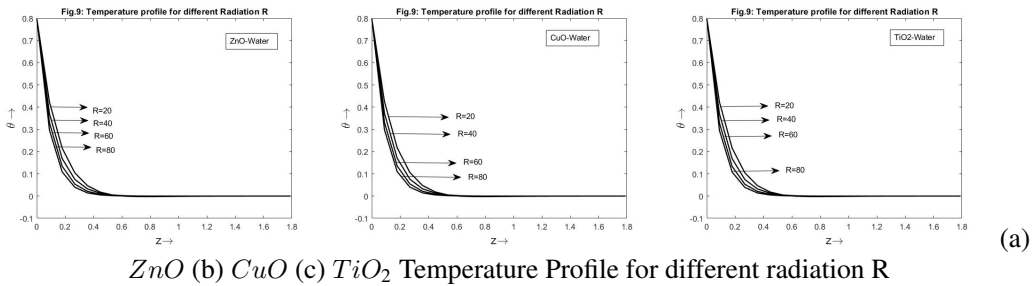


Figure 9 displays the temperature profiles for different values of the radiation parameter ( $R$ ), under the conditions  $Pr = 6.2$ ,  $t = 0.8$ , and  $\phi = 0.1$ . It is observed that the temperature of the nanofluid decreases as the radiation parameter ( $R$ ) increases.

Figure 10 illustrates that the temperature of the nanofluid increases with an increase in time ( $t$ ).



## 4 Conclusion

The objective of this study is to analyze the unsteady rotating flow of a nanofluid past an oscillating vertical plate with variable temperature, considering the effects of thermal radiation. Using the Laplace transform, a closed-form solution for the plate velocity is derived for three distinct types of nanofluids. The influence of various parameters on the velocity profiles is graphically illustrated, and the key findings can be summarized as follows:

- When the phase angle ( $\omega t$ ) decreases, the primary velocity ( $u$ ) increases.
- When the phase angle ( $\omega t$ ) increases, the secondary velocity ( $v$ ) increases.
- If the radiation parameter ( $R$ ) increases, the primary velocity ( $u$ ) increases.
- If the radiation parameter ( $R$ ) increases, the secondary velocity ( $v$ ) increases.
- If the rotation parameter ( $\Omega$ ) decreases, the primary velocity ( $u$ ) increases.
- If the rotation parameter ( $\Omega$ ) decreases, the secondary velocity ( $v$ ) increases.

More study is required to better understand how nanoparticle concentration, size, and shape affect radiative heat transfer efficiency and overall thermal performance. Additionally, for different kinds of nanoparticles, such as  $SiO_2$ ,  $MnO$ , and  $Fe_2O_3$ , as well as for different base fluids, including oil and ethylene glycol, the effects of rotation and oscillation on radiative heat transfer should be investigated.

## References

- [1] E. ABU-NADA, *Effect of nanofluid variable properties on natural convection in enclosures*, International Journal of Thermal Sciences, **49**, 479–491 (2010) <https://doi.org/10.1016/j.ijthermalsci.2009.09.002>
- [2] E. ABU-NADA, F. HAKAN, OZTOP, I. POP, *Buoyancy induced flow in a nanofluid filled enclosure partially exposed to forced convection*, Superlattices and Microstructures, Vol. **51**, pp. 381-395 (2012) <https://doi.org/10.1016/j.spmi.2012.01.002>
- [3] S. Dilip jose, and A.selvaraj, *Effects of Parabolic Flow Past an Accelerated Isothermal vertical Plate with heat and Mass Diffusion in the presence of Rotation*, International Journal of Aquatic Science, Vol. **12**, Issue 03, (2021). ISSN: 2008-8019.
- [4] A. Akbarinia, M. Abdolzadeh, R. Laur, *Critical investigation of heat transfer enhancement using nanofluids in microchannels with slip and non-slip flow regimes*, Appl Therm Eng, Vol **31**, pp. 556-565 (2011) <https://doi.org/10.1016/j.applthermaleng.2010.10.017>

- [5] S. Sarala, E. Geetha, and M. Nirmala, *Numerical investigation of heat transfer and hall effects on mhd nanofluid flow past over an oscillating plate with radiation*, Journal of Thermal Engineering, Vol. **8**, No. 6 pp. 1–15 (2022) <https://doi.org/10.18186/thermal.1201859>
- [6] Asmaa H. Dhiaa, Marwa A. Salih, Hayder A. Al-Yousefi *Effect of ZnO Nanoparticles on the Thermo-Physical Properties and Heat Transfer of Nano-Fluid Flows*, International Journal of Heat and Technology, Vol. **38**, No. 3, September, 2020, pp. 715-721. <https://doi.org/10.18280/ijht.380316>
- [7] Ravikumar J and Vijayalakshmi A.R, *Exact solution of vertical plate in a rotating fluid with variable temperature and mass diffusion in the presence of thermal radiation*, Global Journal of Pure and Applied Mathematics, Vol. **12**, No.2, ISSN 0973-1768 (2016)
- [8] S.U.S. Choi, *Nanofluids: from vision to reality through research*, Journal of Heat Transfer, Vol. **131**, 2009, pp. 1-9 <https://doi.org/10.1115/1.3056479>
- [9] T. Elango, A. Kannan, and K. Kalidasa Murugavel, *Performance study on single basin single slope solar still with different water nanofluids*, Desalination Vol.**360**, March 2015, pp. 45–51. <https://doi.org/10.1016/j.desal.2015.01.004>
- [10] S. Das, R. N. Jana, and O. D. Makinde, *Magneto hydrodynamic free convective flow of nanofluids past an oscillating porous flat plate in a rotating system with thermal radiation and hall effects*, Journal of Mechanics, Vol. **32**, No. 2 (2016) <https://DOI.org/10.1017/jmech.2015.49>
- [11] Nirmal Kumar Kund, *Numerical Modeling for Thermal Investigations of Fuel Cell by Using TiO<sub>2</sub>, ZnO and SiO<sub>2</sub> Water Based Nanofluids*, International Journal for Research in Applied Science and Engineering Technology (IJRASET), Vol. **5** Issue X, October 2017, ISSN: 2321-9653. <http://doi.org/10.22214/ijraset.2017.10253>
- [12] Soran M. Mamand, *Thermal Conductivity Calculations for Nanoparticles Embedded in a Base Fluid*, MDPI applied sciences, Vol. **11**, No.4, 2021, 1459. <https://doi.org/10.3390/app11041459>
- [13] D.Y. Tzou, *Thermal instability of nanofluids in natural convection*, International Journal of Heat and Mass Transfer, Vol. **51**, pp 2967-2979 (2008) <https://doi.org/10.1016/j.ijheatmasstransfer.2007.09.014>
- [14] E. Geetha, R. Muthucumaraswamy, M. Kothandapani, *Effects of thermal radiation on an unsteady nanofluid flow past over a vertical plate*, International Journal of Pure and Applied Mathematics, Vol. **113** No. 9, 38-46 (2017)
- [15] E. Jothi, A. Selvaraj, S. Dilipjose, A. Neel Armstrong, and S. Karthikeyan, *Effect of MHD and Radiation Absorption Fluid Flow Past an Exponentially Accelerated Vertical Plate with Variable Temperature and Concentration*, Proceedings of First International Conference on Mathematical Modeling and Computational Science, Vol. **1292**, May 2021, pp 429–439. [https://doi.org/10.1007/978-981-33-4389-4\\_39](https://doi.org/10.1007/978-981-33-4389-4_39)
- [16] D. Iranian, and P. Loganathan, *Unsteady Free Convection Flow of a Nanofluid Over a Moving Vertical Plate with Constant Heat and Mass Flux*, International Review of Mechanical Engineering, Vol. **16**, No.1 2022. <https://doi.org/10.15866/ireme.v16i1.21720>
- [17] D. Iranian, J. Manigandan, and Ilyas Khan, *Double diffusive hydromagnetic natural convection of hybrid nanofluid (TiO<sub>2</sub>-Cu/Water) over an infinite vertical plate with viscous dissipation and thermal radiation*, Journal of Thermal Analysis and Calorimetry, Vol. **148**, 2023, pp 10319–10334. <https://doi.org/10.1007/s10973-023-12399-4>
- [18] J. Manigandan, D. Iranian, Ilyas Khan, Najla A. Mohammed, and Hadil Alhazmi, *Numerical simulations of thermal heat conservation in hybrid nanofluids with chemical reaction, viscous dissipation, and inclination*, Case Studies in Thermal Engineering, Vol. **58**, June 2024. <https://doi.org/10.1016/j.csite.2024.104386>

### Author information

A. Antony Gnana Aravind, Department of Mathematics, Faculty of Engineering and Technology, SRM Institute of Science and Technology, Vadapalani Campus, No.1 Jawaharlal Nehru Salai, Vadapalani, Chennai-600026, Tamil Nadu., India.  
E-mail: [aa8447@srmist.edu.in](mailto:aa8447@srmist.edu.in)

J. Ravikumar, Department of Mathematics, Faculty of Engineering and Technology, SRM Institute of Science and Technology, Vadapalani Campus, No.1 Jawaharlal Nehru Salai, Vadapalani, Chennai-600026, Tamil Nadu., India.  
E-mail: [ravikumj@srmist.edu.in](mailto:ravikumj@srmist.edu.in)